1-2018

Presence of Cofactor NADPH Slows Down the Dissociation of Methotrexate from Dihydrofolate Reductase from Bacillus stearothermophilus

Ryan Seamus Foley
Montclair State University

ABSTRACT

The goal of this project was to study the effect of the presence or absence of the cofactor NADPH on the binding and release of ligand methotrexate (MTX) to/from *Bacillus stearothermophilus* (*Bs*) dihydrofolate reductase (DHFR). A previously developed, fluorescently-labeled *Bs* DHFR (C73A/S131CMDCC DHFR) was used to investigate the kinetics and protein conformational motions associated with the binding of NADPH and the binding of methotrexate to the holoenzyme. This *Bs* DHFR contains a distal cysteine where the fluorophore, N-[2-(1-maleimidyl)ethyl]-7-(diethylamino)coumarin-3-carboxamide (MDCC) can be covalently attached. This probe is sensitive to the local molecular environment, reporting on changes in the protein conformation associated with ligand binding. Intrinsic tryptophan fluorescence of the unlabeled *Bs* DHFR construct (C73A/S131C DHFR) was also used to detect changes in conformational motion upon ligand and cofactor association and dissociation.

Previous stopped-flow data indicates the presence of two native state *Bs* DHFR conformers that bind to ligand at different rates. Similarly, two conformations of *Escherichia coli* DHFR in unbound state were reported. Intrinsic tryptophan fluorescence of C73A/S131C *Bs* DHFR and probe fluorescence of C73A/S131CMDCC *Bs* DHFR both report on ligand binding. The labeled and unlabeled DHFRs report on the two different conformers, respectively. This study shows that NADPH binding significantly slows down the dissociation rate (approx. 1000-fold) of methotrexate from *Bs* DHFR from 0.015 ±0.007965 s^{-1} to 0.000021 ±0.00000271 s^{-1}. This demonstrates the importance of NAHPH in the analysis and study of DHFR.

MONTCLAIR STATE UNIVERSITY

PRESENCE OF COFACTOR NADPH SLOWS DOWN THE DISSOCIATION OF METHOTREXATE FROM DIHYDROFOLATE REDUCTASE FROM *BACILLUS STEAROTHERMOPHILUS*

By

Ryan S. Foley

A Master's Thesis Submitted to the Faculty of

Montclair State University

In Partial Fulfillment of the Requirements

For the Degree of

MASTER OF SCIENCE

January 2018

College of Science and Mathematics

Department Chemistry and Biochemistry

Thesis Committee:

[redacted]

Dr. Nina M. Goodey
Thesis Sponsor

[redacted]

Dr. John Siekierka
Committee Member

[redacted]

Dr. David Talaga
Committee Member

PRESENCE OF COFACTOR NADPH SLOWS DOWN THE DISSOCIATION OF METHOTREXATE FROM DIHYDROFOLATE REDUCTASE FROM *BACILLUS STEAROTHERMOPHILUS*

A THESIS

Submitted in partial fulfillment of the requirements

For the degree of Master of Science

by

RYAN SEAMUS FOLEY

Montclair State University

Montclair, NJ

2018

Table of Contents:

List of Figures:

Introduction:

Dihydrofolate reductase (DHFR) is an essential enzyme found in nearly all life forms. DHFR catalyzes the formation of tetrahydrofolate from dihydrofolate using the cofactor NADPH as the reducing agent. Tetrahydrofolate is required in the synthesis of purines, thymidylate and several amino acids and reducing its activity prevents cells from growing or multiplying. This makes DHFR an important pharmaceutical target for development of antibiotics and pharmaceuticals targeting cancer [41, 42]. Pharmaceuticals that inhibit DHFR's function are known as antifolates [19]. Studying how these drugs interact with DHFR is important for further research into protein dynamics and the design of new pharmaceuticals.

DHFR has become one of the main model systems for studying protein conformational motions [10]. Enzymes are thought to exist in a variety of conformations that are in equilibrium with each other. For many enzymes, one conformer is the stable state; for others, more than one stable conformer exists in equilibrium [13, 27]. An enzyme that exists in multiple stable conformers has the possibility of more elaborate regulation. Studies on how one conformer as opposed to the other binds ligands leads to a better understanding of potential regulation [1, 8, 9, 24].

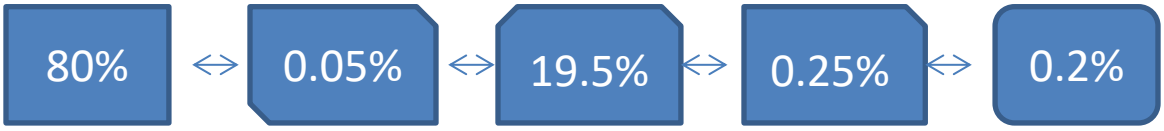

Figure 1: A visualization of how enzyme conformers exist in many conformations with a prominent few conformations that are most stable.

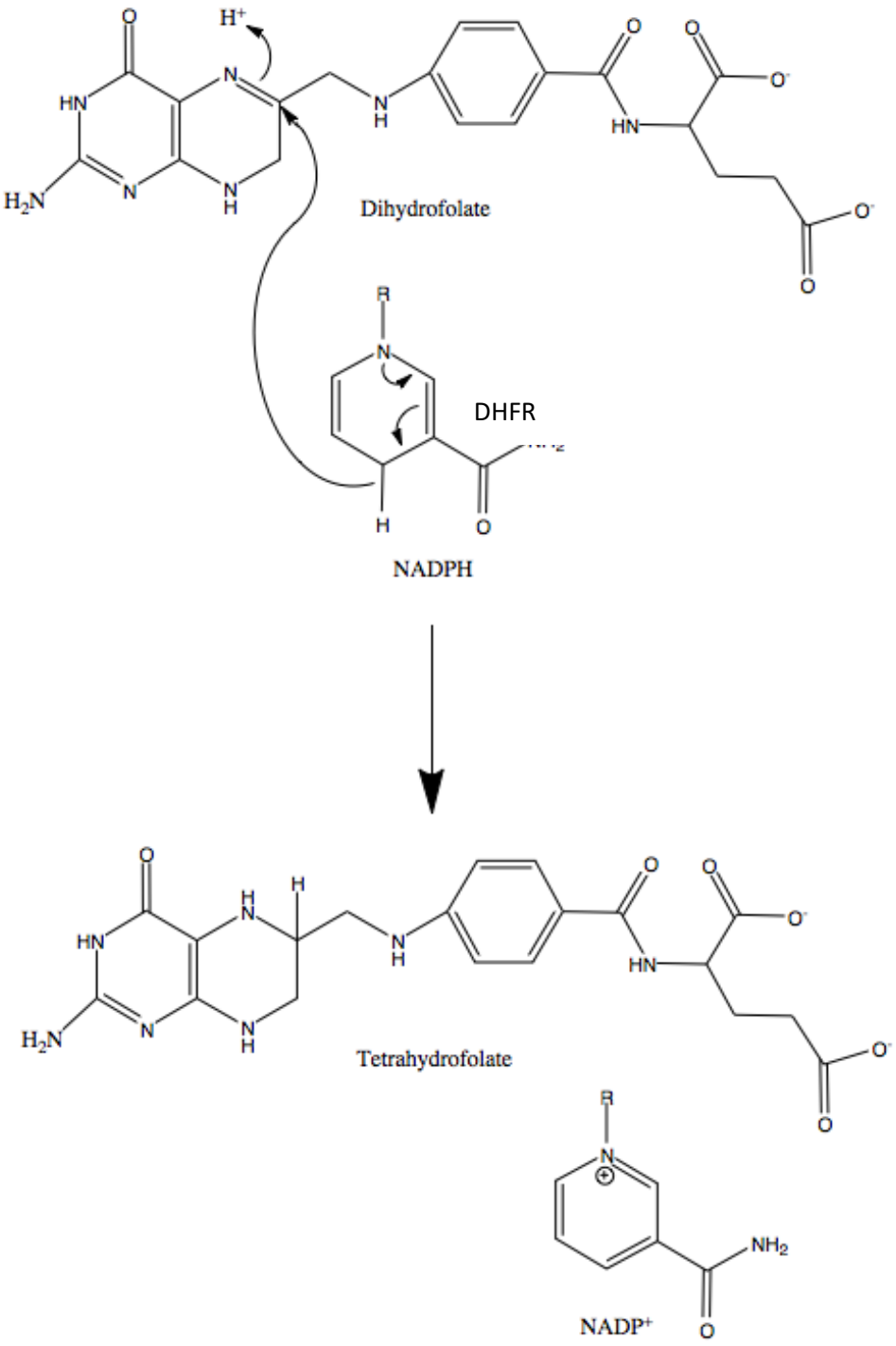

Figure 2: The reaction of Dihydrofolate to Tetrahydrofolate by Dihydrofolate Reductase using NADPH as a cofactor.

Previous published work on DHFR has demonstrated at least two stable conformations that bind ligands at different rates [30]. A confounding factor of this system is the cofactor NADPH. Most research has focused on the apoenzyme (enzyme without cofactor bound), presumably to avoid the complexity of the bound cofactor. As a result, less is known about the binding of methotrexate (MTX) to the holoenzyme (enzyme with cofactor bound). However, the holoenzyme needs to be studied because it is the biologically relevant species. Understanding the interactions between DHFR, NADPH, and methotrexate will increase the understanding of structure function relationships in DHFR. Thus, the goal is to determine the extent to which NADPH impacts the binding of DHFR to methotrexate and the associated conformational dynamics. There are three specific goals:

- Find rates of binding and dissociation and associated conformational changes of methotrexate binding to *Bs* DHFR.
- Determine the rates of binding and dissociation of NADPH to/from *Bs* DHFR and rates of associated conformational changes.
- Determine the rate of methotrexate binding to the *Bs* DHFR holoenzyme (with NADPH bound), rate of release of methotrexate from holoenzyme, and rates of associated conformational changes.

Stopped-flow fluorescence spectroscopy was used to determine rates of binding, dissociation and associated conformational changes. This method measures changes in fluorescence intensity over time after two fluid flows are mixed together. The measurement begins as the flows are stopped. The dead time of the instrument is approximately one to two milliseconds. In this project, I measured changes in the

intensity of the intrinsic tryptophan fluorescence for the unlabeled enzyme. I measured changes in the fluorescence intensity of the covalently bound fluorophore MDCC for the labeled enzyme. In both measurements, the intensity of the fluorophore signal will change when the conformation of the *Bs* DHFR changes. This is because the environment of the fluorophore changes when the protein undergoes a conformational change.

Integrating these two fluorescence signals allowed me to differentiate between binding events associated with each conformer. Each of the two conformers may have different biding mechanisms to methotrexate. For example, one conformer may bind faster than the other or release methotrexate more rapidly. There may also be conformational changes that are associated with the methotrexate binding event or ones that follow the binding event for one or both conformers. At low methotrexate concentrations, concentration dependent binding steps can be seen the best. At higher methotrexate concentrations, the concentration dependent binding steps are so fast they are over in the dead time of the instrument, allowing the slower concentration independent conformational changes to be measured clearly. With these tools, we determined the rates of binding events and conformational changes for the binding of NADPH and methotrexate to both the apoenzyme, the enzyme without its cofactor NADPH, and the holoenzyme, the enzyme with the cofactor NADPH bound.

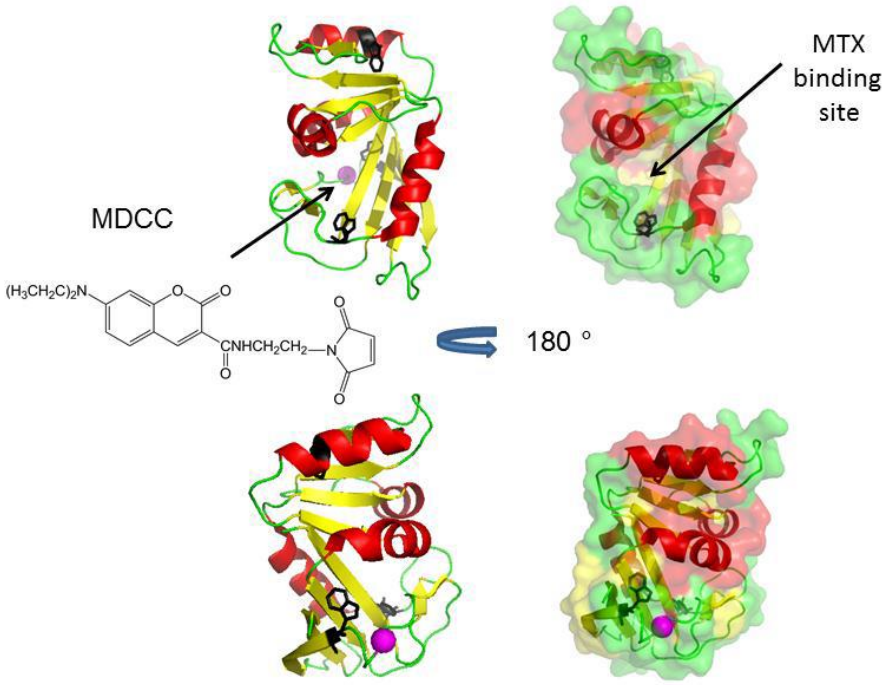

Figure 3: A graphical representation of the structure of *Bs* DHFR (PDB ID: 1ZDR) [1]. These models show the front (top) where the MTX binding site is located and the back (bottom) where the MDCC fluorescent probe gets attached. Residue 131, the site of labeling, is shown as a magenta sphere.

Material and methods

Protein expression and purification

An *E. coli* BL21 cell line transformed with C73A S131C *Bs* DHFR with the was obtained from a previous study done by Maryam Alapa [1]. The unlabeled *Bs DHFR* construct (C73A/S131C *Bs* DHFR) was grown and expressed in LB broth containing 100 µg/mL ampicillin at 37 °C. OD_{600} was allowed to reach 0.6; expression was then induced using 1 mM isopropyl-β-D-thiogalactopyranoside (IPTG) and the cells expressed overnight at 30 °C. Cells were washed in 0.9% NaCl and pelleted.

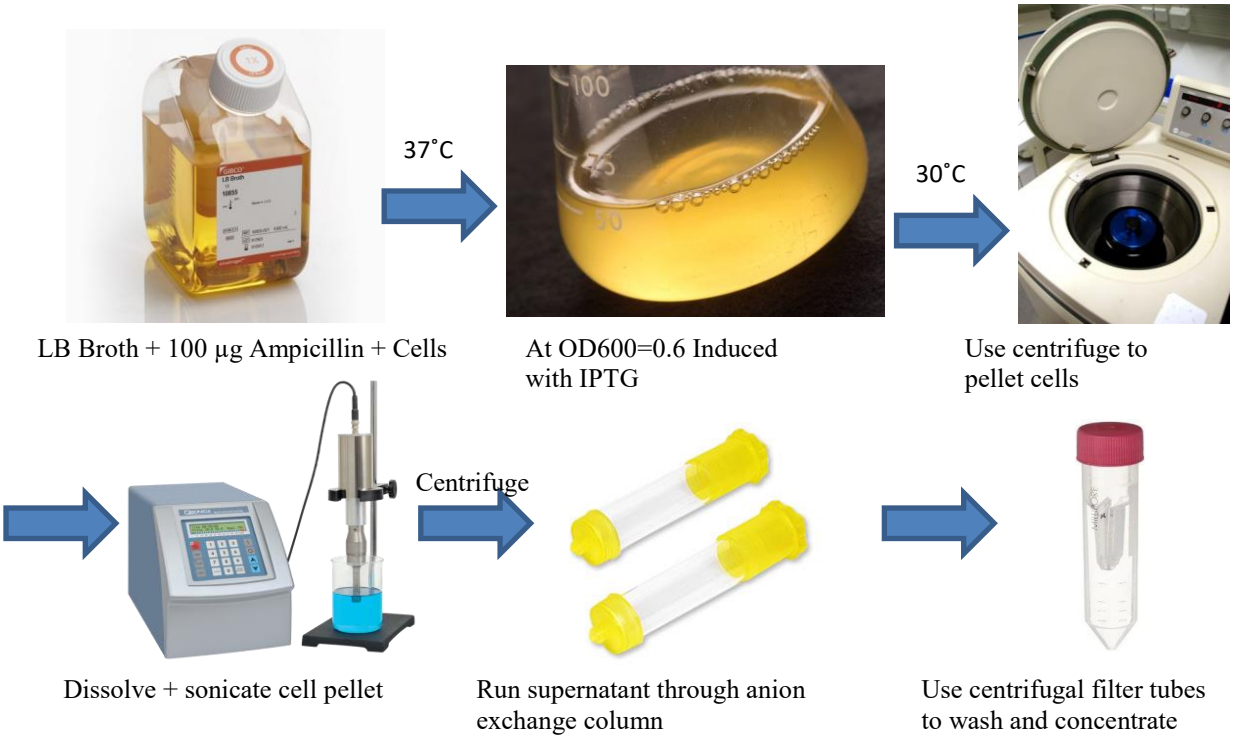

Figure 4: Process figure for the growth and purification of C73A S131C *Bs* DHFR.

The cells were suspended in 40 mM *N*-2-hydroxyethylpiperazine-*N*'-2-ethanelsulfonic acid (HEPES) buffer at pH 6.8, then lysed by sonication at 10% duty with an output of 5 pulsed for 4 minutes. The supernatant was loaded onto an SP-sepharose C-25 column and eluted with 0.2 M NaCl in 40 mM HEPES (pH 6.8). The *Bs* DHFR fractions were collected, exchanged into 40 mM HEPES (pH 6.8), concentrated, and stored at -80 °C with a typical yield of 2.5 mg of protein for 1 L of Expressed protein broth. The purity was verified by SDS-PAGE electrophoresis.

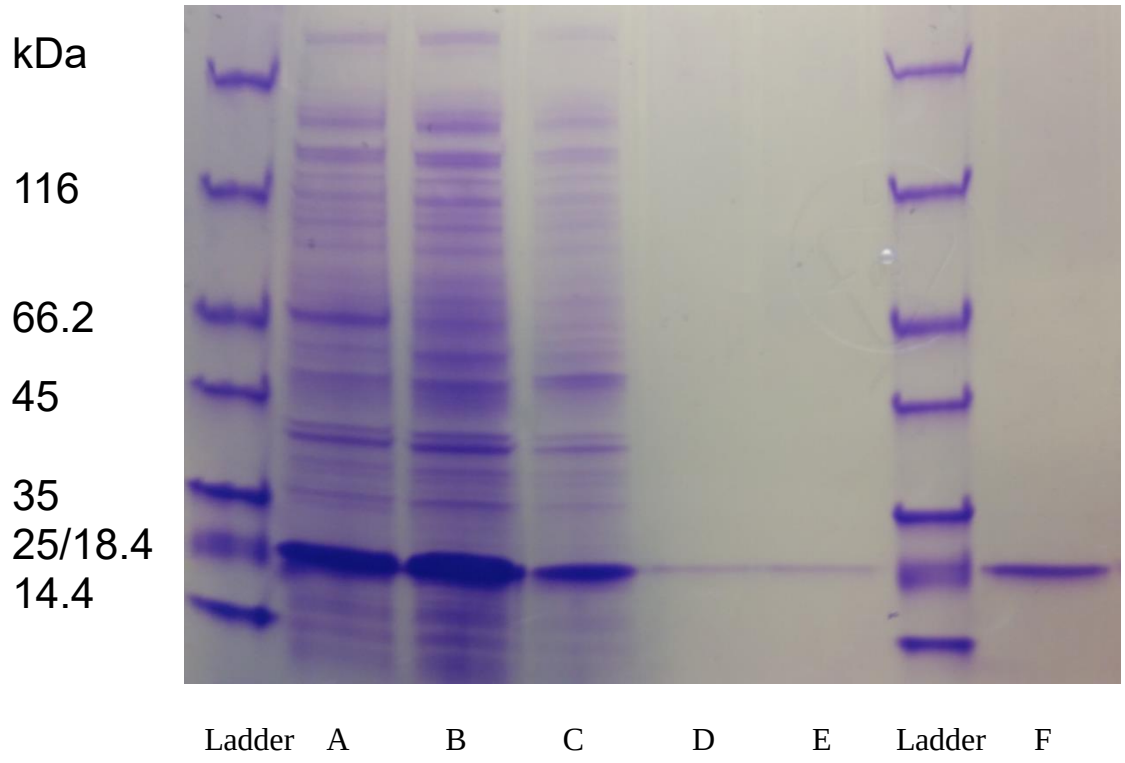

Figure 5: This is a typical gel for the purification of C73A/S131C *Bs* DHFR using a SP-sepharose C-25 column. The molecular weight of *Bs DHFR* is 18.6 kDa A) lysate, B) flow column 1, C) flow column 2, D) eluted DHFR 1, E) eluted DHFR 2, F) concentrated DHFR (approximately 0.002 mg) at very high purity.

Preparation of C73A/S131CMDCC Bs DHFR

Covalent attachment of the MDCC fluorophore to cysteine on the *Bs* DHFR complex at position 131 was initiated by adding a 3-fold molar excess of 0.22 mM stock solution of MDCC fluorophore (ThermoFisher Scientific, Catalog number: D10253, 7-Diethylamino-3-((((2-Maleimidyl)ethyl)amino)carbonyl)coumarin, MW 383.4 g/mol), dissolved in dimethyl sulfoxide, to purified C73A/S131C *Bs* DHFR in pH 7.2 HEPES buffer. The final concentrations were 139.1 μM of MDCC and 41.5 μM of *Bs* DHFR with

a final volume of 1.65 mL. The mixture was covered with aluminum foil to protect the sample from light and incubated at room temperature for 2 h. The sample was dialyzed twice, once for 4 h at 4 °C and once overnight at 4 °C in HEPES pH 6.8 to remove excess dye and to exchange buffer. The extinction coefficient of DHFR (25,565 $M^{-1}cm^{-1}$ at 280 nm) and of MDCC (10,000 $M^{-1}cm^{-1}$ at 280 nm and 50,000 $M^{-1}cm^{-1}$ at 419 nm) were used to calculate labeling efficiency. Labeling efficiency was found to be ~99.4 % from absorbance measurements at 280 and 419 nm using a Thermo Scientific NanoDrop 2000c UV-Vis spectrophotometer.

Absorption = Extinction coefficient * Concentration * Distance

	(M^{-1} cm^{-1})	(M)	(cm)
A280 DHFR	25565		0.1
A280 MDCC	10000		0.1
A419 MDCC	50000		0.1

Figure 6: This shows the equation and constants used in the calculation of enzyme concentration, amount of MDCC needed for the labeling, and the labeling efficiency. Labeling efficiency is calculated by comparing the concentration calculation of MDCC at 419 nm to the concentration calculation of DHFR at 280nm (subtracting out the A280 of MDCC from the total). Sample calculation Fig. 19 in Appendix.

Unlabeled apoenzyme Bs DHFR mixed with methotrexate

Methotrexate (2–200 μM) was mixed with 2 μM of C73A/S131C *Bs* DHFR in 50 mM 2-(*N*-morpholino) ethanesulfonic acid, 25 mM tris(hydroxymethyl)-aminomethane, 25 mM ethanolamine, and 100 mM NaCl (MTEN buffer) at pH 7 in an Applied Photophysics SX20 stopped-flow apparatus. The changes in fluorescence emission

intensity for C73A/S131C *Bs* DHFR (excitation at 290 nm, emission with a 320 nm cutoff filter) were recorded in the stopped-flow apparatus (slit widths 1 mm) for 0.25 – 500 s. Five individual traces were used to obtain an average trace for each condition. Control data for responses were obtained by taking fluorescence readings of each component when separately when combined in the stopped-flow apparatus with buffer. For example, to determine the contribution of DHFR to the fluorescence of the DHFR/MTX experiment, DHFR was mixed in the stopped-flow cell with buffer and the fluorescence measured.

To measure the dissociation rate of the DHFR-MTX complex, 2 μM enzyme was incubated with 10 μM methotrexate in MTEN buffer at pH 7. The enzyme-methotrexate solution was then mixed in a stopped-flow apparatus with 300 μM or 700 μM trimethoprim (TMP) which displaces methotrexate in the active site. The dissociation event was monitored by following the fluorescence emission changes at 320 nm for 500s.

To further explore the dissociation rate of the DHFR-MTX complex a concentration of 1 μM enzyme, 5 μM methotrexate, and 700 μM trimethoprim (TMP) in MTEN buffer at pH 7 was mixed (TMP mixed in immediately prior to fluorescence readings) and placed in a Flouromax SX20 spectrophotometer. The dissociation event was monitored by following the fluorescence emission changes at 320 nm for 600s and 172800s (48h).

Labeled apoenzyme Bs DHFR mixed with methotrexate

Methotrexate (2– 200 μM) was mixed with 2 μM of C73A/S131C$_{MDCC}$ *Bs* DHFR in MTEN buffer at pH 7 in the stopped-flow apparatus. The changes in fluorescence

emission intensity for C73A/S131C$_{MDCC}$ (excitation at 419 nm, emission with a 450 nm cutoff filter) were recorded in the stopped-flow apparatus (slit widths 1 mm) for 0.25-500s. Five individual traces were used to obtain an average trace for each condition. Control data for responses were obtained by taking fluorescence readings of each component separately when combined in the stopped-flow apparatus with buffer.

To measure the dissociation rate of the DHFR-MTX complex, 2 μM enzyme was incubated with 10 μM methotrexate in MTEN buffer at pH 7. The enzyme-methotrexate solution was then mixed in a stopped-flow apparatus with 300 μM or 700 μM TMP to displace methotrexate. The dissociation event was monitored by following the fluorescence emission changes at 450 nm for 500s.

To further explore the dissociation rate of the DHFR-MTX complex a concentration of 1 μM enzyme, 5 μM methotrexate, and 700 μM trimethoprim (TMP) in MTEN buffer at pH 7 was mixed (TMP mixed in immediately prior to fluorescence readings) and placed in a Flouromax SX20 spectrophotometer. The dissociation event was monitored by following the fluorescence emission changes at 450 nm for 600s and 172800s (48h)

Unlabeled apoenzyme Bs DHFR mixed with NADPH

NADPH (2–200 μM) was mixed with 2 μM of C73A/S131C *Bs* DHFR in MTEN buffer at pH 7 in the stopped-flow apparatus. The changes in fluorescence emission intensity for C73A/S131C *Bs* DHFR (excitation at 290 nm, emission with a 320 nm cutoff filter) were recorded in the stopped-flow apparatus (slit widths 1 mm) for 0.25-500s. Five individual traces were used to obtain an average trace for each condition.

Control data for responses were obtained by taking fluorescence readings of each component separately when combined in the stopped-flow apparatus with buffer.

Labeled apoenzyme Bs DHFR mixed with NADPH

NADPH (2– 200 μM) was mixed with 2 μM of C73A/S131C$_{MDCC}$ *Bs* DHFR in MTEN buffer at pH 7 in the stopped-flow apparatus. The changes in fluorescence emission intensity for C73A/S131C$_{MDCC}$ (excitation at 419 nm emission with a 450 nm cutoff filter) were recorded in the stopped-flow apparatus (slit widths 1 mm) for 0.25-500s. Five individual traces were used to obtain an average trace for each condition. Control data for responses were obtained by taking fluorescence readings of each component separately when combined in the stopped-flow apparatus with buffer.

Unlabeled holoenzyme Bs DHFR mixed with methotrexate

Methotrexate (2– 200 μM) was mixed with 2 μM of C73A/S131C *Bs* DHFR, pre-incubated with 10 μM NADPH, in MTEN buffer at pH 7 in the stopped-flow apparatus. The changes in fluorescence emission intensity for C73A/S131C *Bs* DHFR (excitation at 290 nm, emission with a 320 nm cutoff filter) were recorded in the stopped-flow apparatus (slit widths 1 mm) for 0.25-500s. Five individual traces were used to obtain an average trace for each condition. Control data for responses were obtained by taking fluorescence readings of each component separately when combined in the stopped-flow apparatus with buffer.

To measure the dissociation rate of the DHFR-NADPH-MTX complex, 2 μM enzyme incubated with 10 μM NADPH was incubated with 10 μM methotrexate in

MTEN buffer at pH 7. The enzyme-methotrexate solution was then mixed in a stopped-flow apparatus with 300 μM or 700 μM TMP to displace methotrexate. The dissociation event was monitored by following the fluorescence emission changes at 320nm for 500s.

To further explore the dissociation rate of the DHFR-NADPH-MTX complex a concentration of 1 μM enzyme, 5 μM NADPH, 5 μM methotrexate, and 700 μM trimethoprim (TMP) in MTEN buffer at pH 7 was mixed (TMP mixed in immediately prior to fluorescence readings) and placed in a Flouromax SX20 spectrophotometer. The dissociation event was monitored by following the fluorescence emission changes at 320 nm for 600s and 172800s (48h)

Labeled holoenzyme Bs DHFR mixed with methotrexate

Methotrexate (2– 200 μM) was mixed with 2 μM of C73A/S131C_{MDCC} *Bs* DHFR pre-incubated with 10 μM NADPH in MTEN buffer at pH 7 in the stopped-flow apparatus. The changes in fluorescence emission intensity C73A/S131C_{MDCC} (excitation at 419 nm, emission with a 450 nm cutoff filter) were recorded in the stopped-flow apparatus (slit widths 1 mm) for 0.25-500s. Five individual traces were used to obtain an average trace for each condition. Control data for responses were obtained by taking fluorescence readings of each component separately when combined in the stopped-flow apparatus with buffer.

To measure the dissociation rate of the DHFR-NADPH-MTX complex, 2 μM enzyme incubated with 10 μM NADPH was incubated with 10 μM methotrexate in MTEN buffer at pH 7. The enzyme-methotrexate solution was then mixed in a stopped-

flow apparatus with 300 μM or 700 μM TMP to displace methotrexate. The dissociation event was monitored by following the fluorescence emission changes at 450 nm for 500s.

To further explore the dissociation rate of the DHFR-NADPH-MTX complex a concentration of 1 μM enzyme, 5 μM NADPH, 5 μM methotrexate, and 700 μM trimethoprim (TMP) in MTEN buffer at pH 7 was mixed (TMP mixed in immediately prior to fluorescence readings) and placed in a Flouromax SX20 spectrophotometer. The dissociation event was monitored by following the fluorescence emission changes at 450 nm for 600s and 172800s (48h)

Data Analysis

Data Analysis was done using Dynafit 4 [23], a minimization fitting program, to do an optimization analysis to fit the data to the following kinetic model. The model for the binding of methotrexate to *Bs* DHFR elucidated by previous studies (Fig. 4) was used as a basis for the Dynafit analysis. For each section of the model, only one, two steps, or pure conformational change step (E+L←→E.L, or E'+L←→E'.L←→E.L or E'.L ←→E.L) were used with the goal of using as few steps as possible to adequately explain each set of the data. Each trace typically shows evidence of only one or two steps with all timescales and wavelength showing the whole picture. Dynafit files and scripts are found in each respective binding folder under the file heading: Dynafit Ready Data Files + Scripts. Binding (k_1) steps were all successfully fit to a one step model and all conformational change (k_2) steps were fit to a simple conformational change step as well as a two step model.

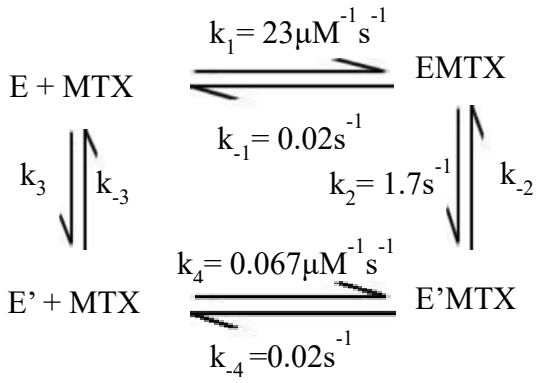

Figure 7: The minimal model for methotrexate binding to *Bs* DHFR. E and E' represent different conformational states of *Bs* DHFR, L represents a ligand (Methotrexate or NADPH in this case), and E.L and E'.L represent different conformational states of *Bs* DHFR bound to a ligand. The rate constants are first order rate constants in units of s^{-1} for the conformational changes and second order rate constant $\mu M^{-1} s^{-1}$ for the ligand binding steps.

Analysis for the data was carried out through an iterative process. Initial estimates for parameters such as enzyme, buffer, and ligand responses (Table 1) were determined from control data. Responses were determined by subtracting out the background fluorescence and dividing by concentration. The control parameters were constantly monitored to prevent significant deviation from measured values. These parameters included the response values for the enzyme alone, the response values for the ligand alone, and the offset which corresponds to the response generated by the buffer alone. Based on rough single exponential analysis of the emission vs. time curves, using multiple concentrations of methotrexate and NADPH mixed with the enzyme, initial parameter estimates for k_1 along with the rough values for the known responses were used to get an initial calculation for the concentration of enzyme (Fig. 8).

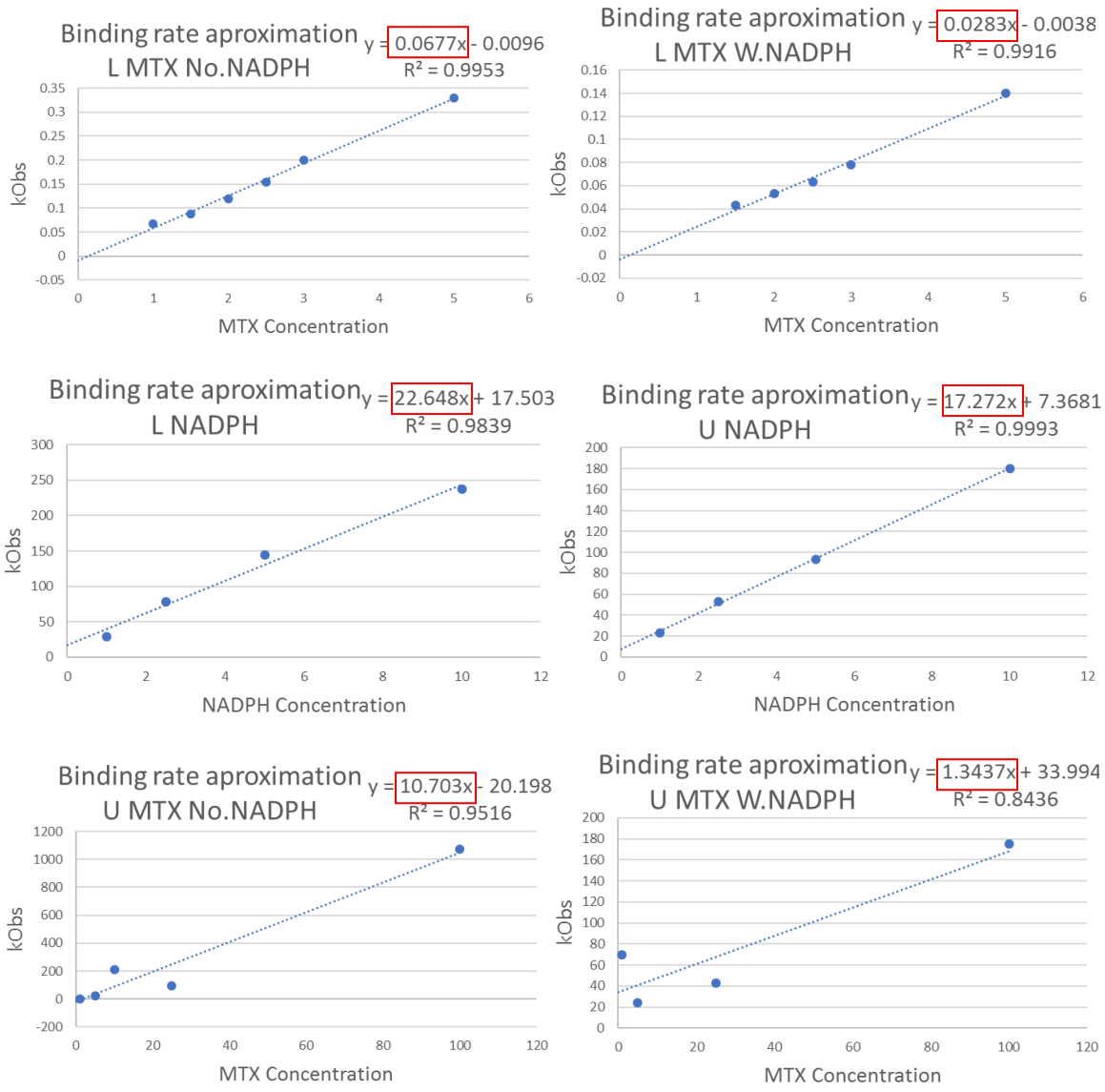

Figure 8: Initial estimates for binding constants. The estimate of the binding constant is indicated by the slope of a best fit linear line through the data (red box). Only the approximation of L MTX W.NADPH was quite far off in terms of precision. This data as well as the calculation of the kObs values for each concentration can be found in **Folder**: kObs graphs and data, within each of the corresponding binding folders.

This concentration reflects the percent of the enzyme that is in the E conformation for binding NADPH through the E+L→EL pathway. This is important for knowing the distribution between E and E' while the total enzyme concentration is known to be 1 μM. With nearly all parameters decently defined, each trace was run through an iterative process where the parameters were allowed to vary individually and in groups as well as all at once to develop a best fit trace for each fitting. The values from these were then used to determine global best fits across data sets.

	NADPH	Binding
	L	U
DHFR	1.92	0.477
NADPH	0.000001	0.0352
DHFR.NADPH	0.965	0.961
DHFR'.NADPH	0.942	0.94

	MTX	Binding		MTX	Binding
	L	U		L	U
DHFR	1.935	0.86	DHFR.NADPH	5.21	0.89
MTX	0.00001	0.001	MTX	0.00001	0.001
DHFR.MTX	0.934	0.756	DHFR.NADPH.MTX	5.1	0.856
DHFR'.MTX	0.746	0.73	DHFR'.NADPH.MTX	5.1	0.83

Table 1: Control values for the Dynafit response constants. Used as initial values and refined through the Dynafit iterative modeling process. **File:** Response Values.

Results and Discussion

Methotrexate Mixed with Bs DHFR

Independently confirming the model of methotrexate binding and the rates at which methotrexate binds to *Bs* DHFR is important for further analysis. Knowing the rates of binding and conformational changes and how they are different for the

DHFR.NADPH system is important for determining NADPH's role in methotrexate binding. Seeing the same previously observed conformational changes researched by Maryam Alapa would ideally confirm the conformational equilibrium in *Bs* DHFR [1].

The binding of methotrexate to unlabeled *Bs* DHFR causes a change in tryptophan fluorescence (290 nm) intensity. There are three tryptophan molecules *(Trp22, Trp85 and Trp135)* in our *Bs* DHFR enzyme, one of which is in the active site. These tryptophan molecules give off varying amounts of fluorescence depending on their local environment. For instance, one can clearly detect change in the fluorescence intensity when a molecule is binding to the active site and detect changes in fluorescence intensity as the protein shifts conformation [1] .

The binding of methotrexate to unlabeled *Bs* DHFR causes a fast methotrexate concentration dependent decrease in tryptophan (290) fluorescence intensity. There is also a second, slower decrease in fluorescence, the rate of which does not vary with methotrexate concentration. The traces were fitted to a two-step equation. The fast concentration dependent decrease is over within 0.25 seconds and has a k_1 of 23.8 ±2.2 $\mu M^{-1} s^{-1}$ and k_{-1} was calculated to be 0.8 ±0.29 s^{-1}. (Table 2) The fast step is attributed to methotrexate binding, k_1, and the slower step is attributed to the conformational change, k_2, as the DHFR-MTX complex moves to equilibrium between its two forms. The rate constant k_2 was found to be 0.02 ±0.0027 s^{-1}. (Table 2) It was not possible to determine k_{-2} from this particular data.

The binding of methotrexate to labeled *Bs* DHFR causes a slower concentration dependent decrease in MDCC fluorescence (419 nm) intensity. The MDCC probe which is attached to the *Bs* DHFR at a distal site is sensitive to small changes in its local

environment changing fluorescence intensity as any binding or conformational changes occur. The traces were fitted to a two-step equation. This is a concentration dependent decrease is over within 100 seconds and has a k_4 of 0.072 ±00013 $\mu M^{-1} s^{-1}$ and a k_{-4} of approximately 0.0064 ±0.000066 s^{-1}. (Table 2)

Longer unlabeled traces showed a slow decrease in fluorescence intensity indicating a slow methotrexate concentration independent decrease. By running these samples at high methotrexate concentrations, the methotrexate concentration dependent step becomes so fast that it cannot be observed on the timescale of our data collection and all that can be seen is the concentration independent step. These longer traces were fit to a two-step model. The fast step is attributed to methotrexate binding (k_1), and the slower step is attributed to the conformational change (k_2) as the DHFR-MTX complex shifts its conformation finding a new conformation equilibrium with different amounts of DHFR being in each conformation. The rate constant k_2 was fond to be 0.02 ±0.0027 s^{-1} and k_{-2} could not be calculated from the data. (Table 2)

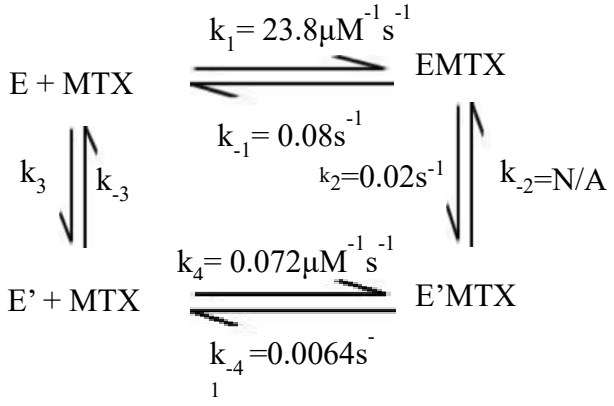

Figure 9: Model for the rates of binding and conformational changes associated with methotrexate binding to the unlabeled *Bs* DHFR and labeled *Bs* DHFR.

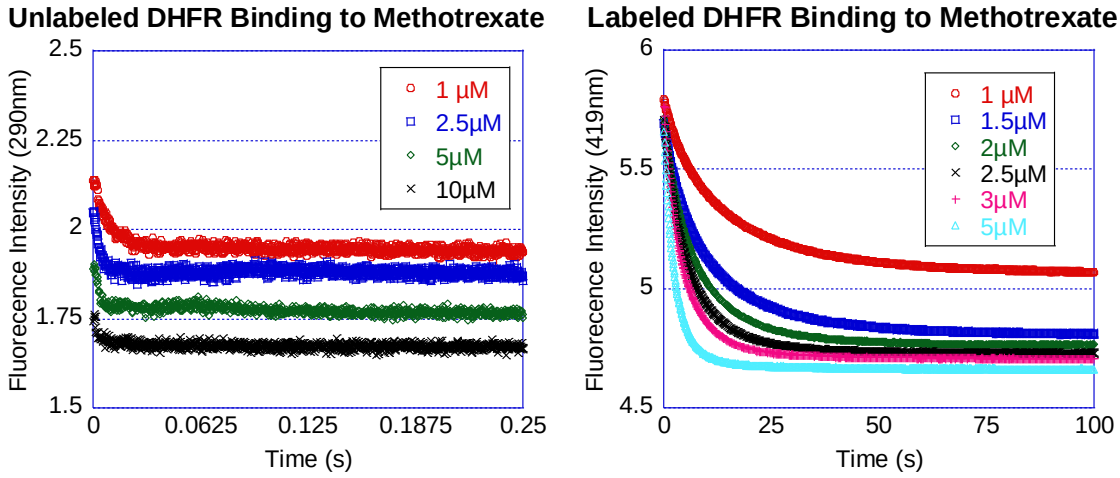

Figure 10: Unlabeled *Bs* DHFR (1 µM) mixed with various concentrations of MTX in MTEN buffer at pH 7 and at 25.7 °C (left). **Data File**: U MTX Binding No.NADPH 0.25s Data. **Data Folder**: U MTX Binding No.NADPH. This shows a fast concentration dependent fluorescence decrease corresponding to the k_1 step of rate 23.8 ±2.2 $\mu M^{-1} s^{-1}$. Labeled *Bs* DHFR (1 µM) mixed with various concentrations of MTX in MTEN buffer at pH 7 and at 25.7 °C (right). **Data File**: L MTX Binding No.NADPH 100s Data. **Data Folder**: L MTX Binding No.NADPH. This shows a much slower concentration dependent fluorescence decrease corresponding to the k_4 step of rate 0.072 ±00013 $\mu M^{-1} s^{-1}$. These analyses were done in Dynafit and the script files are located in the Dynafit Ready Data Files + Scripts folder within each relevant binding folder. These very different rates at two distinct timescales that are both concentration dependent is what indicates that there are two separate conformers binding at separate rates. This pattern was previously determined in prior research by Maryam Alapa [1]. Maryam Apala's research yielded two k_1 of 20.2 ±0.21 $\mu M^{-1} s^{-1}$ and 23.99 ±1.9 $\mu M^{-1} s^{-1}$ and a k_4 of 0.067 ±0.0001 $\mu M^{-1} s^{-1}$. These values are very close matches to my own.

Unlabeled 0.25s	Average	Standard Error
k_1	23.8 μM^{-1} s^{-1}	2.2
k_{-1}	0.8 s^{-1}	0.29
Unlabeled 100s		
k_2	0.02 s^{-1}	0.0027
k_{-2}	N/A	N/A
Labeled 100s		
k_4	0.072 μM^{-1} s^{-1}	0.00013
k_{-4}	0.0064 s^{-1}	0.000066

Table 2. Rates of binding and conformational changes associated with methotrexate binding to the unlabeled *Bs* DHFR and labeled *Bs* DHFR. Based on Dynafit calculation of and averaged 3-5 traces per concentration and 3-5 concentrations per rate. **Data Folders:** U MTX Binding No.NADPH, L MTX Binding No.NADPH. The script files are in the Dynafit Ready Data Files + Scripts folder within each relevant binding folder.

Methotrexate binding to *Bs* DHFR can be modeled as two separate, two step processes. This implies that *Bs* DHFR is a dynamic system. Based on this and previous studies *Bs* DHFR like many enzymes is not rigid and at equilibrium is most often found in two forms (E and E'). The separate conformations of *Bs* DHFR bind methotrexate at different rates and the motions that *Bs* DHFR goes through after ligand binding (E+L→E.L and E'+L→E'L) can conform to a model where *Bs* DHFR undergoes a conformational change after binding takes place (EL → EL').

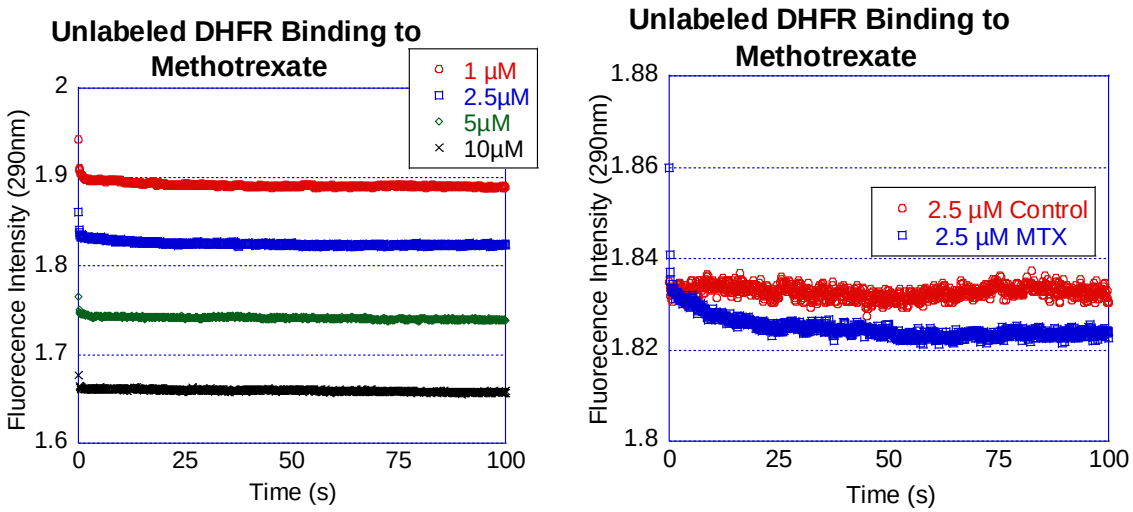

Figure 11: Unlabeled *Bs* DHFR (1 µM) mixed with various concentrations of MTX in MTEN buffer at pH 7 and at 25.7 °C (left). **Data File**: U MTX Binding No.NADPH 100s Data. **Data Folder**: U MTX Binding No.NADPH. This shows a slow concentration independent fluorescence decrease that can be attributed to the k_2 step of rate 0.02 ±0.0027 s^{-1} which is a conformational change. Unlabeled *Bs* DHFR (1 µM) mixed 2.5 µM of MTX in MTEN buffer at pH 7 and at 25.7 °C, control sample was premixed for 5 minutes (right). **Data File**: U MTX Binding No.NADPH 100s Data +control. **Data Folder**: U MTX Binding No.NADPH. The control run is mixed together and allowed to bind and settle into its conformations before reading its value providing a constant value with which the conformational change, which can often be subtle, can be more clearly visualized. The right graph zooms in and shows the conformational change.

NADPH Mixed with Bs DHFR

Determining how NADPH binds to *Bs* DHFR and what changes in conformation take place is important for clarifying our understanding of the NADPH/MTX/DHFR system. Seeing conformational changes in the DHFR.NADPH complex would suggest

that the conformational equilibrium in DHFR vs. the DHFR.NADPH system are different and should be treated differently.

The binding of NADPH to unlabeled *Bs* DHFR causes an NADPH concentration dependent increase in tryptophan fluorescence (290 nm) intensity. The traces were fitted to a single step model. This is a fast concentration dependent increase and is over within 0.2 seconds and has a k_1 of 19.5 ±0.18 μM^{-1} s^{-1} and a k_{-1} of 3.9 ±0.11 s^{-1}. (Table 3)

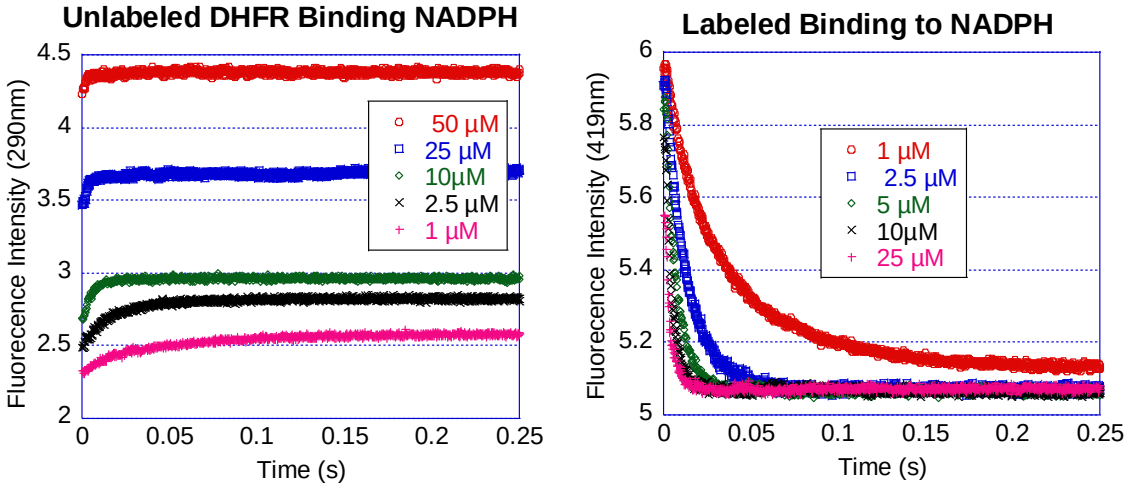

Figure 12: Unlabeled *Bs* DHFR (1 µM) mixed with various concentrations of NADPH in MTEN buffer at pH 7 and at 25.2 °C (left). **Data File**: U NADPH Binding 0.25s Data. **Data Folder**: U NADPH Binding. This shows a fast concentration independent fluorescence increase that can be attributed to the k_1 step of rate 19.5 ±0.18 μM^{-1} s^{-1}. Labeled *Bs* DHFR (1 µM) mixed with various concentrations of NADPH in MTEN buffer at pH 7 and at 25.2 °C (right). **Data File**: L NADPH Binding 0.25s Data. **Data Folder**: L NADPH Binding. This shows a fast concentration independent fluorescence decrease that can be attributed a k_4 step of rate 35.6 ±0.11 $\mu M^{-1} s^{-1}$.

The binding of NADPH to labeled *Bs* DHFR causes a NADPH concentration dependent decrease in MDCC fluorescence intensity. The traces were fitted to a single step equation. This is a fast concentration dependent decrease is over within 0.25 seconds and has a k_4 of 35.6 ±0.15 $\mu M^{-1} s^{-1}$ and a k_{-4} of near 0 s^{-1}. (Table 3)

Longer unlabeled traces showed a small decrease in fluorescence intensity indicating a slow NADPH concentration independent decrease. These longer traces were fit to a two-step model. The fast step is attributed to NADPH binding, k_1, and the slower step is attributed to the conformational change, k_2. The rate constant k_2 was found to be 0.02 ±0.0002 s^{-1} and k_{-2} could not be calculated from the data.

Longer labeled traces showed a small decrease in fluorescence intensity indicating a slow NADPH independent decrease. These longer traces were fit to a single step model of a conformational change. The rate constant k_{-2} was fond to be 0.1 ±0.0041 s^{-1} and k_2 was unable to be calculated from the data. (Table 3)

NADPH binding to *Bs* DHFR, like methotrexate, can be modeled with two conformers binding ligand at different rates. It is likely that *Bs* DHFR existing as two conformers (E and E') bind NADPH at different rates and the motions that *Bs* DHFR goes through after ligand binding (E+L→E.L and E'+L→E'L) can conform to a model where *Bs* DHFR undergoes a conformational change after binding takes place (EL → EL').

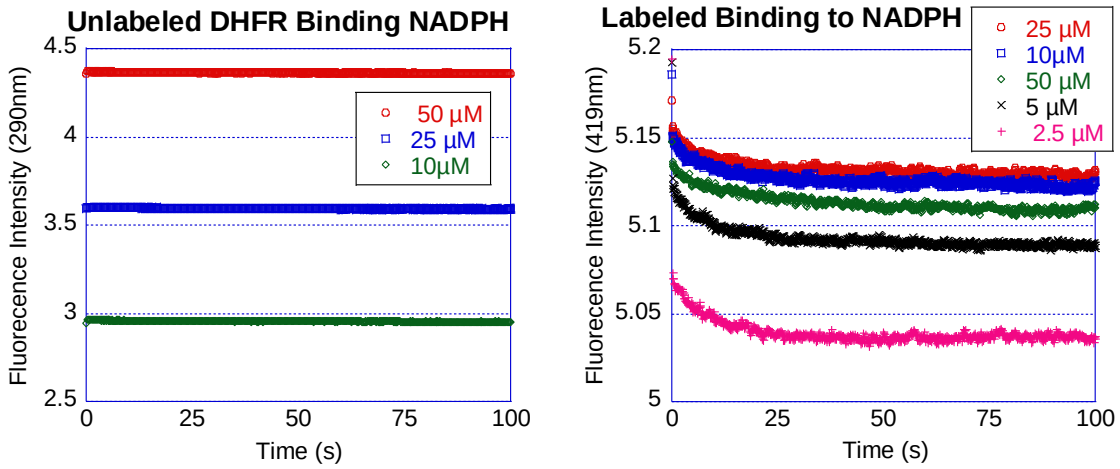

Figure 13: Unlabeled *Bs* DHFR (1 µM) mixed with various concentrations of NADPH in MTEN buffer at pH 7 and at 25.2 °C (left). **Data File**: U NADPH Binding 100s Data. **Data Folder**: U NADPH Binding. This shows a slow concentration independent fluorescence decrease that can be attributed to the k_2 step of rate 0.02 ±0.0002 s^{-1} which is a conformational change. Unlabeled *Bs* DHFR (1 µM) mixed with various concentrations of NADPH in MTEN buffer at pH 7 and at 25.2 °C (right). **Data File**: L NADPH Binding 100s Data. **Data Folder**: L NADPH Binding. This shows a concentration independent fluorescence decrease that can be attributed to the k_{-2} step of rate 0.01 ±0.0041 s^{-1} which is a conformational change.

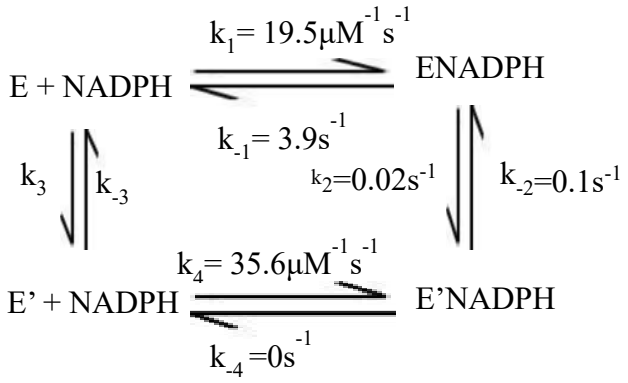

Figure 14: Model with the rates of binding and conformational changes associated with NADPH binding to the unlabeled *Bs* DHFR and labeled *Bs* DHFR.

Unlabeled 0.25s	Rate	Standard Error
k_1	$19.5\mu M^{-1}s^{-1}$	0.18
k_{-1}	$3.9s^{-1}$	0.11
Unlabeled 100s		
k_2	$0.02\ s^{-1}$	0.0002
Labeled 100s		
k_{-2}	$0.1\ s^{-1}$	0.0041
Labeled 0.25s		
k_4	$35.6\ \mu M^{-1}s^{-1}$	0.15
k_{-4}	$0\ s^{-1}$	0.023

Table 3. Rates of binding and conformational changes associated with methotrexate binding to the unlabeled *Bs* DHFR and labeled *Bs* DHFR. Based on Dynafit calculation of and averaged 3-5 traces per concentration and 3-5 concentrations per rate. **Data Folders:** U NADPH Binding, and L NADPH Binding. The script files are in the Dynafit Ready Data Files + Scripts folder within each relevant binding folder.

Methotrexate mixed with DHFR/NADPH Holoenzyme

Finally determining the differences in binding of ligands like methotrexate bind to the DHFR/NADPH holoenzyme complex can clarify the role of NADPH in *Bs* DHFR methotrexate binding and the importance of NADPH to the study and analysis of inhibitors. A significant change in binding, conformational equilibrium, and/or dissociation rate would be a clear indication of the importance NADPH being included in the analysis process.

The binding of methotrexate to unlabeled holoenzyme causes a methotrexate concentration dependent decrease in tryptophan fluorescence intensity (Fig. 14 left). The traces were fitted to a single step model. This is a fast concentration dependent increase and is over within 0.25 seconds and has a k_1 of 24.7 ±1.1 μM^{-1} s^{-1} and a k_{-1} of 0.03 ±0.4 s^{-1}. (Table 4)

The binding of methotrexate to labeled holoenzyme causes a methotrexate concentration dependent decrease in MDCC fluorescence intensity (Fig. 14 right). The traces were fitted to a single step equation. This is a much slower concentration dependent decrease and is over within 100 seconds and has a k_4 of 0.052 ±0.024 $\mu M^{-1} s^{-1}$ and a k_{-4} of 0.03 ±0.01 s^{-1}. (Table 4)

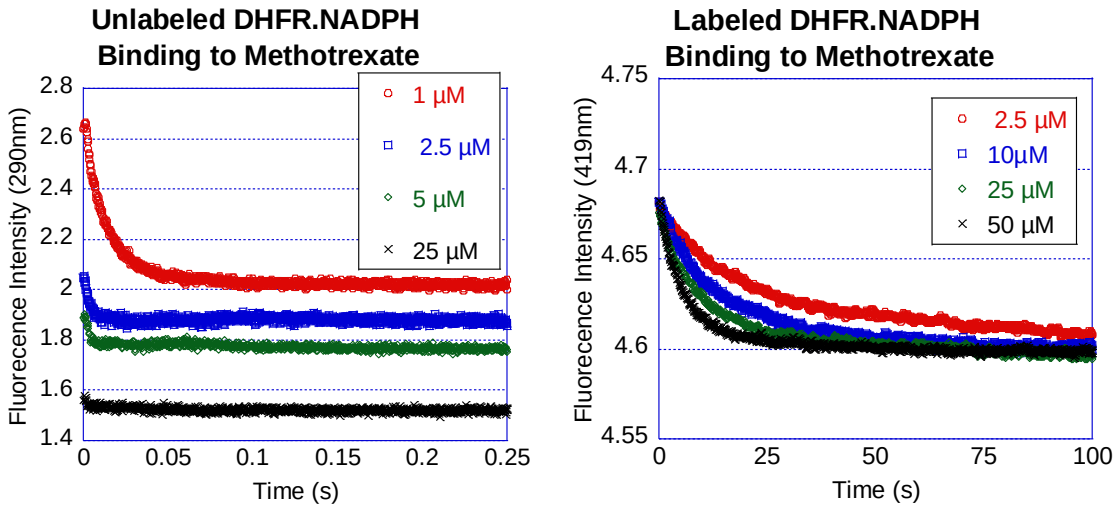

Figure 15: Unlabeled *Bs* DHFR (1 µM) premixed with NADPH (5 µM) and then mixed with various concentrations of MTX in MTEN buffer at pH 7 and at 25.7 °C (left). **Data File**: U MTX Binding W.NADPH 0.25s Data. **Data Folder**: U MTX Binding W.NADPH. This shows a fast concentration dependent fluorescence decrease corresponding to the k_1 step of rate 24.7 ±1.1 μM^{-1} s^{-1}. Labeled *Bs* DHFR (1 µM) premixed with NADPH (5 µM) and then mixed with various concentrations of MTX in MTEN buffer at pH 7 and at 25.7 °C (right). **Data File**: L MTX Binding W.NADPH 100s Data. **Data Folder**: L MTX Binding W.NADPH This shows a much slower concentration dependent fluorescence decrease corresponding to the k_4 step of rate 0.052 ±0.024 $\mu M^{-1} s^{-1}$.

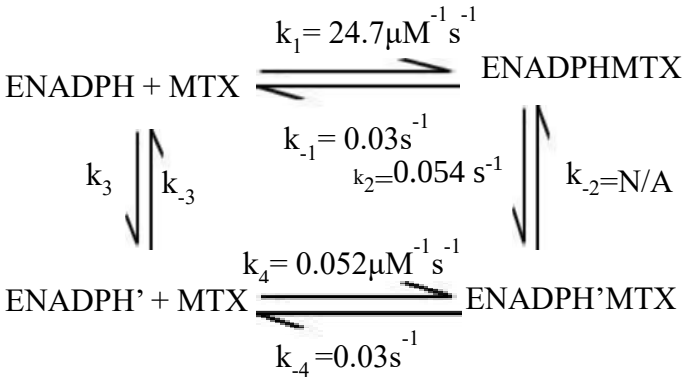

Figure 16: Model for the rates of binding and conformational changes associated with methotrexate binding to the unlabeled DHFR.NADPH complex and labeled DHFR.NADPH complex.

Unlabeled 0.25s	Average	Standard Error
k_1	24.7 $\mu M^{-1}s^{-1}$	1.1
k_{-1}	0.03 s^{-1}	0.4
Unlabeled 100s		
k_2	0.054 s^{-1}	0.0019
k_{-2}	N/A	N/A
Labeled 100s		
k_4	0.052 $\mu M^{-1}s^{-1}$	0.024
k_{-4}	0.03 s^{-1}	0.01

Table 4. Rates of binding and conformational changes associated with methotrexate binding to the unlabeled DHFR.NADPH complex and labeled *Bs* DHFR.NADPH complex. Based on Dynafit calculation of and averaged 3-5 traces per concentration and 3-5 concentrations per rate. **Data Folders:** U MTX Binding W.NADPH, L MTX Binding W.NADPH. The script files are in the Dynafit Ready Data Files + Scripts folder within each relevant binding folder.

Dissociation rates of methotrexate from Bs DHFR and the DHFR.NADPH complex

Determining the differences in the dissociation of ligands like methotrexate from *Bs* DHFR and the DHFR.NADPH complex can clarify the role of NADPH in *Bs* DHFR methotrexate binding and the importance of NADPH to the study and analysis of inhibitors. A significant change in dissociation, indicates an importance of the cofactor in not just activating the enzyme but preventing ligands from dissociating.

The dissociation of methotrexate from unlabeled *Bs* DHFR causes a decrease in tryptophan fluorescence intensity (Fig. 16 left). The rates were calculated an exponential decay model. This shows a fluorescence decrease corresponding to the dissociation rate of 0.015 s^{-1} ±0.007965.

The dissociation of methotrexate from labeled *Bs* DHFR causes an increase in tryptophan fluorescence intensity (Fig. 16 right). The rates were calculated an exponential rise model. This shows a fluorescence increase corresponding to the dissociation rate of 0.02 s^{-1} ±0.0000921.

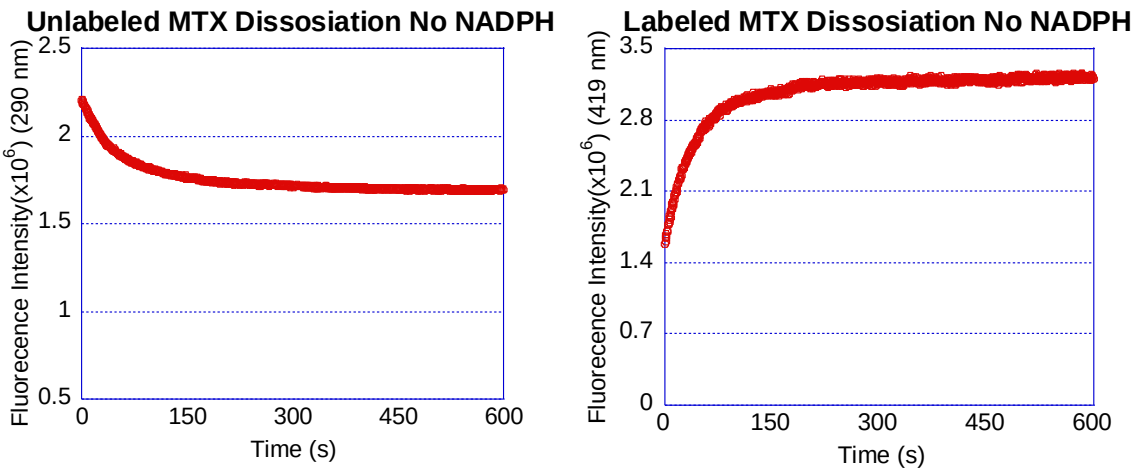

Figure 17: Unlabeled *Bs* DHFR (1 μM) premixed with methotrexate (5 μM) mixed with trimethoprim (TMP 700 μM) in MTEN buffer at pH 7 and at 25.2 °C (left). **Data File**: U MTX Dissociation No NADPH Data. **Data Folder**: U MTX Dissociation No.NADPH. This shows a fluorescence decrease corresponding to the dissociation rate of 0.015 s^{-1} ±0.007965. Labeled *Bs* DHFR (1 μM) premixed with methotrexate (5 μM) and then mixed with trimethoprim (TMP 700 μM) in MTEN buffer at pH 7 and at 25.2 °C (right). **Data File**: L MTX Dissociation No NADPH Data. **Data Folder**: L MTX Dissociation No.NADPH. This shows a fluorescence increase corresponding to the dissociation rate of 0.02 s^{-1} ±0.0000921.

The dissociation of methotrexate from the unlabeled DHFR.NADPH complex causes a decrease in tryptophan fluorescence intensity (Fig. 17 left). The rates were calculated an exponential decay model. This shows a fluorescence decrease corresponding to the dissociation rate of 2.87e^{-5} s^{-1} ±0.82 e^{-}5.

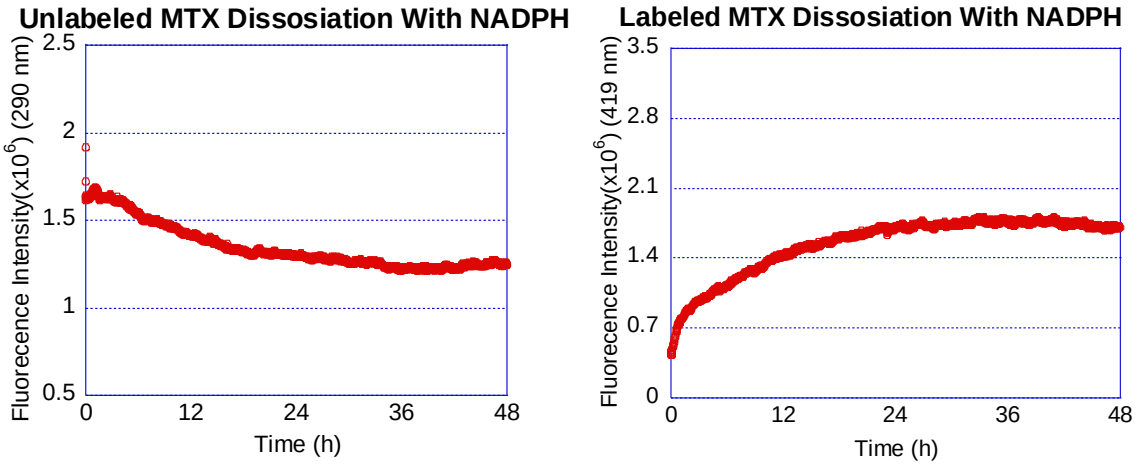

Figure 18: Unlabeled *Bs* DHFR (1 μM) premixed with methotrexate (5 μM) mixed with trimethoprim (TMP 700 μM) in MTEN buffer at pH 7 and at 25.2 °C (left). **Data File**: U MTX Dissociation With NADPH Data. **Data Folder**: U MTX Dissociation W.NADPH. This shows a fluorescence decrease corresponding to the dissociation rate of $2.87e^{-5}$ s^{-1} ±0.82 $e^{-}5$. Labeled *Bs* DHFR (1 μM) premixed with methotrexate (5 μM), and NADPH (5 μM), and then mixed with trimethoprim (TMP 700 μM) in MTEN buffer at pH 7 and at 25.2 °C (right). **Data File**: Labeled MTX Dissociation With NADPH Data. **Data Folder**: L MTX Dissociation W.NADPH. This shows a fluorescence increase corresponding to the dissociation rate of $2.1e^{-5}$ s^{-1} ±0.271 e^{-5}. This specific dissociation curve for the labeled enzyme had irregularities that appeared in the control experiment. (run 48 hours without NADPH) The control was used in file L MTX Dissociation W.NADPH and was subtracted from the average dissociation curve to correct for the irregularities.

The dissociation of methotrexate from the labeled DHFR.NADPH complex causes an increase in tryptophan fluorescence intensity (Fig. 17 right). The rates were

calculated an exponential rise model. This shows a fluorescence increase corresponding to the dissociation rate of $2.1e^{-5}$ s^{-1} ± 0.271 e^{-5}.

Discussion

Previously determined experimental results were verified by our experiments and the kinetic data is consistent with previously determined models for methotrexate binding. We confirmed that *Bs* DHFR exists in two distinct configurations E and E' at a ratio of 0.7:0.3. We have extended scope of the model to include the cofactor NADPH binding resulting in a ENADPH and E'NADPH ratio of 0.6:0.4. This multistep model is supported by the distinct NADPH and methotrexate binding rates calculated from tryptophan fluorescence and the MDCC fluorophore fluorescence. Furthermore, the model is valid when methotrexate binding to the holoenzyme is determined following NADPH bindings.

The difference in rate of methotrexate binding between the apoenzyme and the holoenzyme is indicative of the importance of the cofactor. However, the most significant change from the binding of *Bs* DHFR to NADPH is that the dissociation rate of methotrexate from the bound complex is reduced. This shift results in an increase in stability. This makes sense from a biological perspective as it ensures that when all components are present in solution that they not only bind to each other at an appropriate speed but also that they remain bound so that they achieve an appropriate reaction rate. The scale of the shift in dissociation rate is very interesting. The dissociation rate of the *Bs* DHFR without cofactor is fast while with cofactor it is 1000 times slower, a drastic decrease (Fig. 18).

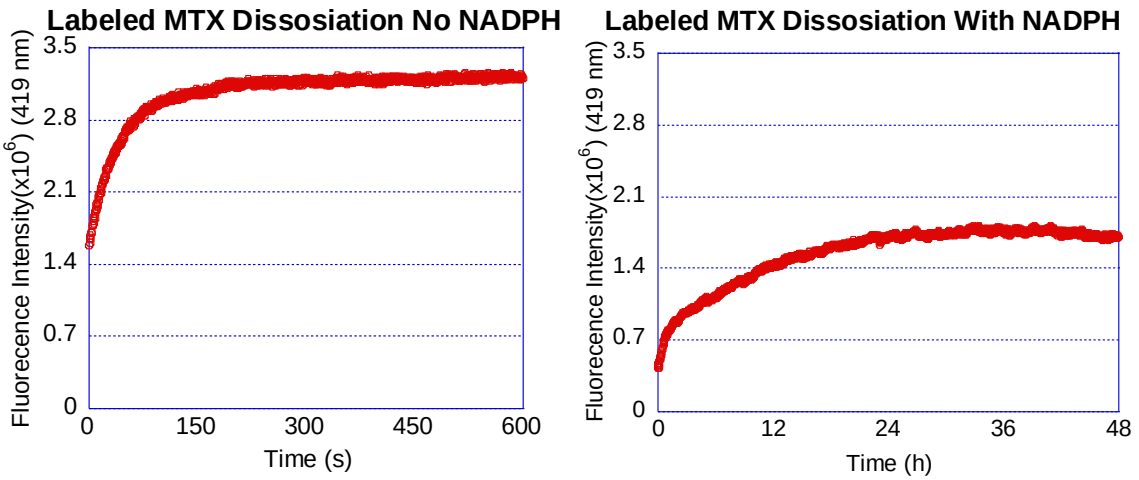

Figure 19: Labeled methotrexate dissociation without NADPH (Fig. 16 right) compared to with NADPH (Fig. 17 right). Here we can clearly visualize the difference in timescale caused by NADPH. When there is no NADPH the timescale for dissociation is 600 seconds with a rate of 0.02 s^{-1} ±0.0000921 and when there is NADPH the timescale for dissociation is 48 hours with a rate of $2.1e^{-5}$ s^{-1} ±0.271 e^{-5}.

We can conclude that important information regarding the kinetics of enzymes and of *Bs* DHFR in particular are missing if the analysis of inhibitor binding data is preformed while a key cofactor is missing. This is especially true when analyzing pharmaceuticals. For example, a cell with high energy (high NADPH concentration) would remain inhibited by methotrexate for much longer than a cell with low energy. This difference could alter effectiveness and toxicity so should be carefully analyzed.

References

1. Alapa, M. T. (2012). Conformational motions associated with ligand binding in dihydrofolate reductase from bacillus stearothermophilus, (master's thesis). Montclair State University, Montclair, NJ
2. Appleman J.R., Howell E.E., Kraut J., Blakley R.L. (1990) Role of aspartate 27 of dihydrofolate reductase from Escherichia coli in interconversion of active and inactive enzyme conformers and binding of NADPH. Journal of Biological Chemistry. 265 55795584.
3. Benkovic, S.J., Hammes-Schiffer, S. (2003) A perspective on enzyme catalysis. Science. 1196-1202.
4. Boehr D.D., McElheny D., Dyson H.J., Wright P.E. (2006) The dynamic energy landscape of dihydrofolate reductase catalysis. Science. 313 1095-9203.
5. Boehr D.D., Nussinov R., Wright P.E. (2009) The role of dynamic conformational ensembles in biomolecular recognition. Nat Chem Biol. 5 789-796
6. Csermely P., Palotai R., Nussinov R., (2010). Induced fit, conformational selection and independent dynamic segments: an extended view of binding events. Nature Proceedings.
7. Eyring H., Polanyi M. (1935) Some applications of the transition state method to calculation of reaction velocities, especially in solution. Trans. Faraday Soc. 31 875-894.
8. Falzone C.J., Wright P.E., Benkovic S.J. (1993) Dynamics of a Flexible Loop in Dihydrofolate Reductase from Escherichia coli and Its Implication for Catalysis. Biochemistry. 33 439-442.
9. Falzone C.J., Wright P.E., Benkovic S.J., (1991) Evidence for Two Interconverting Protein Isomers in the Methotrexate Complex of Dihydrofolate Reductase from Escherichia coli. Biochemistry. 30 2184-2191.
10. Goodey N.M., Alapa M.T., Hagmann D.F., Korunow S.G., Mauro A.K., Kwon K.S., Hall S.M. (2011) Development of a fluorescently labeled thermostable DHFR for studying conformational changes associated with inhibitor binding. Biochem Biophys Res Commun. 413 442-447
11. Goodey N.M., Benkovic S.J. (2008) Allosteric regulation and catalysis emerge via a common route. Nature Chemical Biology. 4 474-482.
12. Goodey N.M., Herbert K.G., Hall S.M., Bagley K.C. (2011) Prediction of residues involved in inhibitor specificity in the dihydrofolate reductase family. Biochem Biophys Acta. 1814 1870-1879.
13. Hammes G., Chang Y.-C., Oas T., (2009) Conformational selection or induced fit: A flux description of reaction mechanism. Proceedings of National Academy of Sciences of the United States of America. 106 13737-13741.
14. Hammes, G.G., Benkovic, S.J., Hammes-Schiffer, S. (2011) Flexibility, diversity, and cooperativity: pillars of enzyme catalysis. Biochemistry. 50 10422-10430

15. Hammes-Schiffer S., Watney J.B. (2006) Hydride transfer catalyzed by Escherichia coli and Bacillus subtilis dihydrofolate reductase: coupled motions and distal mutations. Philos Trans R Soc Lond B Biol Sci. 361 1365-1373.
16. Hatzakis N.S. (2014) Single molecule insights on conformational selection and induced fit mechanism. Biophys Chem. 186 46-54.
17. Hecht D., Tran J., Fogel G.B. (2011) Structural-based analysis of dihydrofolate reductase evolution. Mol Phylogenet Evol. 61 212-230.
18. Horiuchi Y., Ohmae E., Tate S., Gekko K. (2010) Coupling effects of distal loops on structural stability and enzymatic activity of Escherichia coli dihydrofolate reductase revealed by deletion mutants. Biochem Biophys Acta. 1804(4):846-55
19. Huennekens F.M., (1994) The methotrexate story: A paradigm for development of cancer chemotherapeutic agents. Advances in Enzyme Regulation. 34397-419.
20. Johnson K., (2008) Role of Induced Fit in Enzyme Specificity: A Molecular Forward/Reverse Switch. Journal of Biological Chemistry. 283 26297-26301.
21. Kim H.S., Damo S.M., Lee S.Y., Wemmer D., Klinman, J.P. (2005) Structure and hydride transfer mechanism of a moderate thermophilic dihydrofolate reductase from Bacillus stearothermophilus and comparison to its mesophilic and hyper thermophilic homologues. Biochemistry. 44 11428-11439.
22. Kompis I., Islam K., Then R., (2005) DNA and RNA synthesis: antifolates. Chemical Reviews. 105 593-620.
23. Kuzmic P., (1996) Program DYNAFIT for the Analysis of Enzyme Kinetic Data: Application to HIV Proteinase, Analytical Biochemistry 237 260-273.
24. Li L., Falzone C.J., Wright P.E., Benkovic S.J. (1992) Functional Role of a Mobile Loop of Escherichia coli Dihydrofolate Reductase in Transition-State Stabilization. Biochemistry. 31 7826-7833.22
25. Limited, A.P. (2006) SX20 Hardware User Guide.
26. Liu, T., Whitten S.T., Hilser V.J. (2006) Ensemble-Based Signatures of Energy Propagation in Proteins: A New View of an Old Phenomenon. PROTEINS: Structure, Function, and Bioinformatics. 62:728–738
27. Mauldin R.V., Carroll M.J., Lee A.L., (2009) Dynamic Dysfunction in Dihydrofolate Reductase Results from Antifolate Drug Binding: Modulation of Dynamics within a Structural State. Structure. 17 386-394.
28. Morrison, J.F. (1969) Kinetics of the reversible inhibition of enzyme-catalyzed reactions by tight binding inhibitors. BIochimica et Biophysica Acta. 185 269-286.
29. Nussinov R., Ma B., Tsai, C.J. (2014) Multiple conformational selection and induced fit events take place in allosteric propagation. Biophys Chem. 186 22-30.
30. Okondo, Marian. (2015). Effects of allosteric mutations on dihydrofolate reductase, (master's thesis). Montclair State University, Montclair, NJ
31. Oyeyemi O., Sours K.M., Lee T., Resing K.A., Ahn N.G., Klinman J.P. (2010) Temperature dependence of protein motions in a thermophilic dihydrofolate reductase and its relationship to catalytic efficiency. Proceedings of National Academy of Sciences of the United States of America. 107 10074-10079.

32. Pan H., Lee J.C., Hilser V.J. (2000) Binding sites in Escherichia coli dihydrofolate reductase communicate by modulating the conformational ensemble. Proceedings of National Academy of Sciences of the United States of America. 97 12020-12025.
33. Patel S., Little M., Goodey N.M. (2014) Allosteric Ligand Specificity Determining Regions in the Dihydrofolate Reductase Family.
34. QIAGEN. (2012) QIAprep® Miniprep Handbook, 2 ed.
35. Rajagopalan R.T., Zhang Z., McCourt L., Dwyer M., Benkovic S.J., Hammes G.G., (2002) Interaction of dihydrofolate reductase with methotrexate: Ensemble and single molecule kinetics. Proceedings of National Academy of Sciences of the United States of America. 99 13481-13486.
36. Rod T.H., Radkiewicz J.L., Brooks C.L. (2003) Correlated motion and the effect of distal mutations in dihydrofolate reductase. Proc Natl Acad Sci. 100 6980-6985.
37. Sasso S.P., Gilli R.M., Sari J.C., Rimet O.S., Briand C.M. (1994) Thermodynamic study of dihydrofolate reductase inhibitor selectivity. Biochemica et Biophysica Acta. 1207 74-79.
38. Sawaya M., Kraut J. (1997) Loop and Subdomain Movements in the Mechanism of Escherichia coli Dihydrofolate Reductase: Crystallographic Evidence. Biochemistry. 36 586603.
39. Schiffer S.H., Benkovic S.J. (2006) Relating Protein Motion to Catalysis. Annual Review of Biochemistry. 75 519-541.
40. Schnell J.R., Dyson H.J., Wright P.E., (2004) Structure, dynamics, and catalytic function of dihydrofolate reductase. Annual Review of Biochemistry. 33 119-140.
41. Schweitzer, B.I., Dicker, A.P., Bertino, J.R. (1990) Dihydrofolate reductase as a therapeutic target. The FASEB Journal. 4 2441-2452.
42. Sharma M., Chauhan P.M. (2012) Dihydrofolate reductase as a therapeutic target for infectious diseases: opportunities and challenges. Future Medicinal Chemistry. 4 1335-1365.
43. Silva D.A., Bowman G., Sosa-Peinado A., Huang X., (2011) A Role for Both Conformational Selection and Induced Fit in Ligand Binding by the LAO Protein. Public Library of Science Computational Biology. 7 e1002054
44. Singh P., Sen A., Francis K., Kohen A. (2014) Extension and limits of the network of coupled motions correlated to hydride transfer in dihydrofolate reductase. J Am Chem Soc. 136 2575-2582.
45. Stone S.R., Morrison J.F. (1982) Kinetic mechanism of the reaction catalyzed by dihydrofolate reductase from Escherichia coli. Biochemistry. 21 3757-3765.
46. Teague S.J., (2003) Implications of Protein Flexibility for Drug Discovery. Nature Reviews. 2 527-541.
47. Verma C.S., Caves L.S., Hubbard R.E., Roberts G.C. (1997) Domain motions in dihydrofolate reductase: a molecular dynamics study. J Mol Biol. 266 776-796.
48. Vogt A.D., Pozzi N., Chen Z., Di Cera E. (2014) Essential role of conformational selection in ligand binding. Biophys Chem. 186 13-21.

Appendix

$$\frac{\boldsymbol{Absorbance}}{\boldsymbol{Extinction\ coefficent}\ (\boldsymbol{M^{-1}cm^{-1}}) * \boldsymbol{\ Path\ length}\ (\boldsymbol{cm})} = \boldsymbol{Concentration}(\boldsymbol{M})$$

$$\frac{\boldsymbol{Absorbance\ L\ Enzyme}\ (\boldsymbol{419\ nm})}{\boldsymbol{Ext.coeff}, (\boldsymbol{50000M^{-1}cm^{-1}}) * \boldsymbol{\ Path\ length}\ (\boldsymbol{0.1cm})} = \boldsymbol{Concentration\ L\ Enzyme}(\boldsymbol{M})$$

$$\boldsymbol{Concentration\ L\ Enzyme}(\boldsymbol{M}) * \boldsymbol{\ Ext.coeff}, (\boldsymbol{10000M^{-1}cm^{-1}}) * \boldsymbol{\ Path\ length}\ (\boldsymbol{0.1cm}) = \boldsymbol{\ Absorbance\ L\ Enzyme}\ (\boldsymbol{280\ nm})$$

$$\boldsymbol{Absorbance\ Total\ Enzyme}\ (\boldsymbol{280\ nm}) - \boldsymbol{Absorbance\ L\ Enzyme}\ (\boldsymbol{280\ nm}) = \boldsymbol{\ Absorbance\ U\ Enzyme}\ (\boldsymbol{280\ nm})$$

$$\frac{\boldsymbol{Absorbance\ U\ Enzyme}\ (\boldsymbol{280\ nm})}{\boldsymbol{Ext.coeff}, (\boldsymbol{25565M^{-1}cm^{-1}}) * \boldsymbol{\ Path\ length}\ (\boldsymbol{0.1cm})} = \boldsymbol{Concentration\ U\ Enzyme}(\boldsymbol{M})$$

$$\frac{\boldsymbol{Concentration\ L\ Enzyme}(\boldsymbol{M})}{\boldsymbol{Concentration\ U\ Enzyme}(\boldsymbol{M}) + \boldsymbol{\ Concentration\ L\ Enzyme}(\boldsymbol{M})} = \boldsymbol{Labeling\ Efficiency}$$

Figure 20: Equation for converting absorbance to concentration and for measuring labeling efficiency. Absorbance of labeled enzyme at 419 nm and of total enzyme at 280 nm are the measured values for calculating labeling efficiency.

A280	=	ext. coeff	C (M)	l cm		
0.14		25565	5.47624E-05	0.1		
			54.76237043	uM		
		0.00125	L	0.068452963	umol	
Label						
mg/ml	mg/mmol	umol/ul	ul		0.068452963	umol enzyme
0.22	383.4	0.000573813	357.8845367		0.205358889	umol label
labeling						
A419 L	=	ext. coeff	C (M)	l cm		
0.189		50000	0.0000378	0.1		
			37.8	uM		
A280 E	=**0.135**	- A280 L				
0.0972		25565	3.80207E-05	0.1		
			38.02073147	uM		
A280 L						
0.0378		10000	0.0000378	0.1		
			37.8	uM		
				0.994194444	labeling	efficiency

Figure 21: Sample calculation sheet of absorbance, needed label concentration, and labeling efficiency using the equations laid out in Fig. 19 **File:** Absorbance Calculation (In the base data folder). Bold values are measured values and the file auto calculates everything else.

Inventory

Box 1 DHFR supplies

A. 2x 0.5mL tube MTX 35.4mM
B. 1x 1.5mL tube MTX 1000uM
C. 1x 1.5mL tube NADPH 1000uM
D. 1x 0.5mL tube TMP 365mM
E. 1x 1.5mL tubes of labeled enzyme
F. 4x 0.5mL tubes of Labeled enzyme 47.29uM
G. 1x 1.5mL tube of transformed *E. coli* cell culture C73A, S131C
H. 3x1.5mL tubes of unlabeled enzyme
I. 1x 1.5mL tube MDCC old Stock
J. 2x 0.5mL tube of MDCC at 0.22mg/mL
K. 4x 0.5mL tube of unknown (variable) concentration of MDCC (contain particulate)

(box #2 was combined into box 1)

Box #3 DHFR pellets

A. 2x Falcon tubes each contain a cell pellet
B. 1x 10 mL tube with DHFR

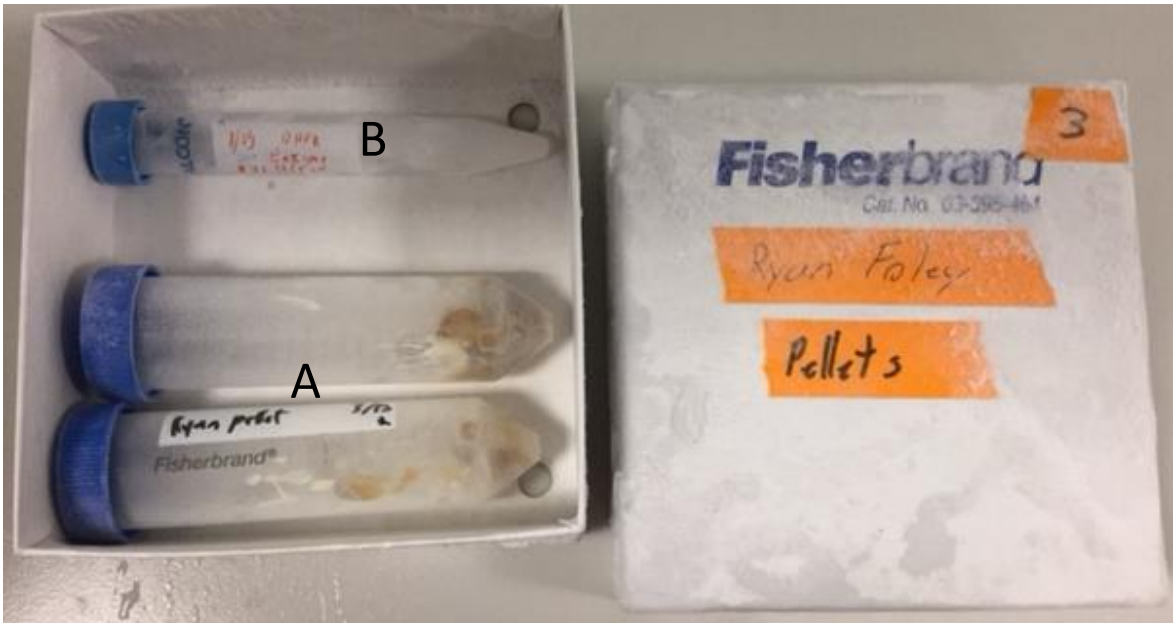

Box 4 Maryam Legacy box

A. Old Pellets from 2012
B. 1x 1.5mL tube of transformed *E. coli* cell culture C73A, S131C

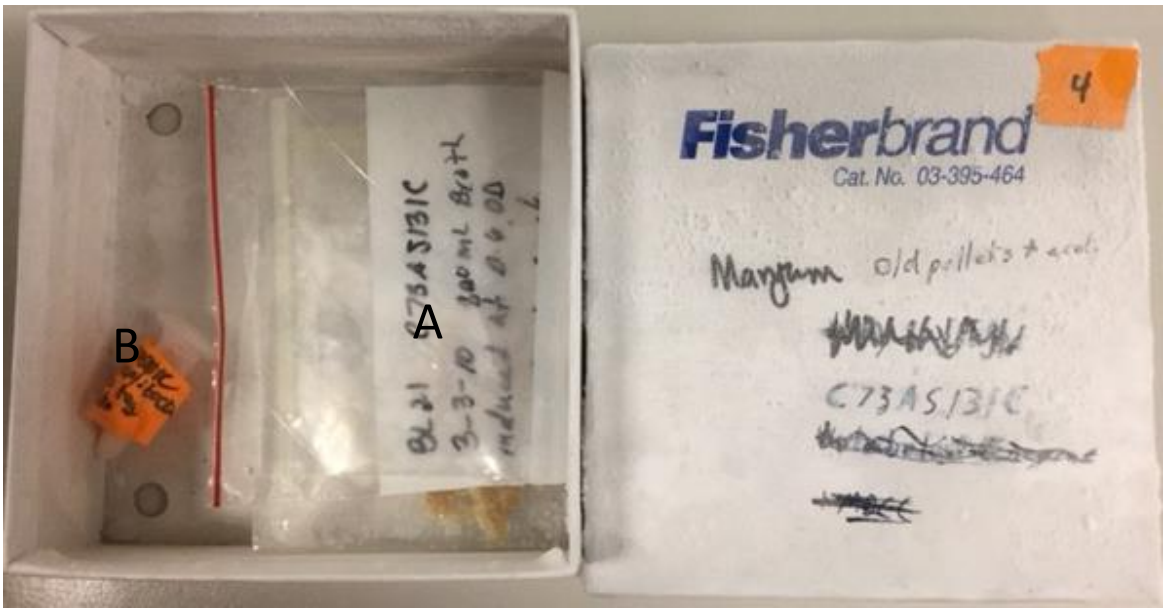

Box 1, 3, 4 in the stand

The stand (A) in the Freezer